Reduction of Quantization Error With Adaptive Wiener Filter in Low Bit Rate Coding

Ching-Chih Kuo, Wen-Thong

Dept. of Communication Engineering, National Chiao-Tung Univ.
Hsinchu, Taiwan, 30050
E-mail: cckuo.cm83g@nctu.edu.tw

ABSTRACT

Wiener filtering is used to reduce the quantization error of the DCT transform coefficients. The process is applied in the transform domain with a sub-band decomposition structure. That is, the corresponding coefficients from each block are grouped together. To model the spectrum of the transform coefficients, two approaches are taken. The first one is to directly estimate the spectrum of the whole sequence. The second one is to remove the dependence among the sequence and model the mean-removed sequence as white noise. With the estimated spectrum, Wiener filter is then used to extract the original coefficients from the quantized ones.

1. INTRODUCTION

With block transform coding, although the transform operation (analysis filter bank and synthesis filter bank) is a perfect-reconstruction (PR) pair, the signal loss is inevitable due to the quantization operation. The results of the quantization are the blocking effect due to coarse quantization of the DC coefficient and the ringing noise, called as the Gibbs phenomenon, due to the coarse quantization of the high frequency subbands. To reduce these effects, one possible solution is redesign of the synthesis filter bank to incorporate the quantizer models to the inverse transform [2] [8] [9]. Other researchers have incorporated the quantization model in the design of filter banks by minimizing the mean square reconstruction error [3] [6]. The resultant filter bank minimizing the overall reconstruction error is also a PR filter bank for Lloyd-Max quantizers. There are also spatial and transform domain post-processing approaches which removes the artifacts of block-transform coded images caused by quantization or channel degradation [7] [8]. In this paper, a post processing is proposed. To remove the quantization noise, Wiener filter is used to process the quantized coefficients. For this, two methods are used to estimate the spectrum of the original un-quantized signal. The first one estimates the spectrum of the whole subband sequence. The second method removes the dependence among the transform coefficients and models the resultant coefficients as white noise. In this approach, the signal spectrum is made a white noise. The second method leads to an adaptive Wiener filter due to the need to adaptively remove the mean for each coefficient. These two filters are applied to different subbands by using the corresponding quantization step size as a parameter for estimating the corresponding quantization noise power.

2. QUANTIZATION PROCESS

To describe the quantization effect, let us denote $f(n_1, n_2)$ and $g(n_1, n_2)$ as the subband signals before and after quantization, respectively. Then, the uniform scalar quantization process is modeled as

$$g(n_1, n_2) = f(n_1, n_2) + v(n_1, n_2) \quad (1)$$

where $v(n_1, n_2)$ is the additive random noise with uniform PDF. That is

$$v(n_1, n_2) \sim U(-\Delta/2, \Delta/2) \quad (2)$$

with Δ being the step size and $U(\cdot)$ representing the uniform PDF.

3. WIENER FILTERING

In this paper we apply the Wiener filtering on each of the quantized subband image and investigate the effect of quantization noise reduction. The purpose of the Wiener filtering is to reduce the blurring effect and to increase the signal-to-noise ratio. The basic requirement when using Wiener filter is to estimate the spectrum of the desired signal. This is the spectrum of the sequence of the corresponding coefficients from all the blocks. In the above, we have mentioned two methods. With the first method, the whole sequence is processed in one time. In this case, the spectrum of the whole sequence is used in the processing. In the second method, we reduce the processing length of the sequence. In the extreme, the

length can be just one point. To process the signal one point at a time, we de-correlate the signal by subtracting the local mean from each point. For the first method, the processing length is chosen to be the same as the window length that is used to calculate the local mean. This length is much shorter than the whole sequence length. In this case, the length of the DFT is N by N, with N =3 or 5. The power spectrum is obtained as the absolute of the square of the DFT. The filter is

$$H(u,v) = (P_s(u,v) - N_q) / P_s(u,v) \qquad (3)$$

The processing result is then

$$P(m,n) = IDFT\{Y_p * H\} \qquad (4)$$

where Y_p is the DFT of the quantized sequence, with

$$P_s(u,v) = |Y_p(u,v)|^2 / N^2 \qquad (5)$$

For the second method [1], it is a little bit more complicated. We have to de-correlate the signal such that we can process them point by point. In the following, we describe the process that we use to de-correlate the signals. Let us denote the additive noise as $v(n_1,n_2)$ and its variance as σ_v^2. For each point in the sequence $f(n_1,n_2)$, we can model it as

$$f(n_1,n_2) = m_f + \sigma_f w(n_1,n_2) \qquad (6)$$

where m_f and σ_f are the mean and standard deviation that are used to describe the point $f(n_1,n_2)$, and $w(n_1,n_2)$ is a zero-mean white noise with unit variance. The point here is that after the mean is removed from the point $f(n_1,n_2)$, the resultant signal is just a white noise. This is what we mean by de-correlation. In this situation, the sequence can be segmented into points and the filtering can be applied point by point. Under this condition, the Wiener filter $H(w_1,w_2)$ is given by

$$H(w_1,w_2) = \frac{P_f(w_1,w_2)}{P_f(w_1,w_2) + P_v(w_1,w_2)} = \frac{\sigma_f^2}{\sigma_f^2 + \sigma_v^2} \qquad (7)$$

From (7), $h(n_1,n_2)$ can be easily derived as a scaled impulse response.

$$h(n_1,n_2) = \frac{\sigma_f^2}{\sigma_f^2 + \sigma_v^2}\delta(n_1,n_2) \qquad (8)$$

This Wiener filtering becomes a point process. All the mean-removed coefficients are processed by a point-mapping transform. The mapping value is a function of the variance. After the mapping, the mean value is added back to generate the desired output. Therefore, the mean value is unchanged during the process. Only the variance is modified. With the subtraction of the mean and modification of the variance and the final add back of the mean grouped together, we derive the following equation, where $p(n_1,n_2)$ is the final output.

$$p(n_1,n_2) = m_f(n_1,n_2) + \frac{\sigma_f^2(n_1,n_2)}{\sigma_f^2(n_1,n_2) + \sigma_v^2} \times \left(g(n_1,n_2) - m_f(n_1,n_2)\right) \qquad (9)$$

with m_f and σ_f^2 updated at each pixel. Note that m_f is identical to m_g when m_v is zero, since only m_g is available. For the determination of the mean, we use a local approach. That is a set of neighboring points is used to estimate the mean. We can estimate $m_f(n_1,n_2)$ in (9) from $g(n_1,n_2)$ by

$$\hat{m}_f(n_1,n_2) = \frac{1}{(2M+1)^2} \sum_{k_1=n_1-M}^{n_1+M} \sum_{k_2=n_{21}-M}^{n_2+M} g(k_1,k_2) \qquad (10)$$

where $(2M+1)^2$ is the number of pixels in the local region used in the estimation. Within the local region, $\sigma_f^2(n_1,n_2)$ can be assumed to be space-invariant. Substituting $\hat{m}_f(n_1,n_2)$ in (10) for $m_f(n_1,n_2)$ in (9) leads to

$$p(n_1,n_2) = g(n_1,n_2) * h(n_1,n_2) \qquad (11)$$

where

$$h(n_1,n_2) = \begin{cases} \dfrac{\sigma_f^2 + \dfrac{\sigma_v^2}{(2M+1)^2}}{\sigma_f^2 + \sigma_v^2}, & n_1 = n_2 = 0 \\ \dfrac{\dfrac{\sigma_v^2}{(2M+1)^2}}{\sigma_f^2 + \sigma_v^2}, & -M \le n_1, n_2 \le M \ \text{ except } n_1 = n_2 = 0 \\ 0, & \text{otherwise} \end{cases}, \qquad (12)$$

This is a time variant filter $h(n_1,n_2)$, because the variance is time variant. Since $\sigma_g^2 = \sigma_f^2 + \sigma_v^2$, σ_f^2 may be estimated from $g(n_1,n_2)$ by

$$\hat{\sigma}_f^2(n_1,n_2) = \begin{cases} \hat{\sigma}_g^2(n_1,n_2) - \sigma_v^2, & \text{if } \hat{\sigma}_g^2(n_1,n_2) > \sigma_v^2 \\ 0, & \text{otherwise.} \end{cases} \qquad (13)$$

where

$$\hat{\sigma}_g^2(n_1,n_2) = \frac{1}{(2M+1)^2} \sum_{k_1=n_1-M}^{n_1+M} \sum_{k_2=n_2-M}^{n_2+M} \left(g(k_1,k_2) - \hat{m}_f(n_1,n_2)\right)^2 \qquad (14)$$

The local mean estimate $\hat{m}_f(n_1, n_2)$ can be obtained from (10), and σ_v^2 is assumed known.

4. SIMULATION RESULTS

In the first experiment, three images "Lena", "Baboon" and "pepper" are used. In the simulation, the 8×8 DCT transform is used as the subband transform of the image coder because of its popularity. After DCT transform of the original image, the coefficients of the same index from each block are grouped to form 64 subband images. Each subband image is then uniform quantized using the quantization table given in the JPEG standard. The coefficients in each subband image are quantized with the same step size since they correspond to the same entry of the quantization table. The results are shown in Table 1,2,3. The ideal spectrum is the spectrum of the un-quantized coefficient. The estimated spectrum is the spectrum of the quantized coefficients. The result indicates that processing with the ideal spectrum is better than that with the estimated spectrum. Also, in both case, the result depends on the size of the window that is used to derive the local mean. In the average, 5 by 5 is a reasonable choice. For cases are studied corresponding to 4 different quantization scale factors. With the estimated spectrum, the improvement is about 0.2. But with ideal spectrum the improvement is about 0.6. This indicate that there is much improvement to be gained if we can have better way to estimate the spectrum. In the second experiment, the "Lenna" image is used as the test image. Here, the quantization scale factor is a parameter for quantization and is chosen to be unity. To test the effectiveness of noise reduction by this method on each subband, the changes of mean square errors of each subband coefficients are computed for uniform scalar quantizers, with support sizes 3×3 and 5×5. The results are presented in Table 4. Note that the 64 subbands are listed in the zig-zag order in these tables. To see the contribution of the quantization noise reduction in the reconstructed image, the reconstructed PSNR of the reconstructed image versus the number of processed subbands (count on zig-zag order) are also computed. The result is presented in Fig. 1. From Table 4, we know that the quantization errors in the lower subbands are effectively reduced for the uniform quantization case. The processsing gain is very low in the high frequency subbands for uniform scalar quantization. From Fig. 1, we know that the reconstructed PSNR's are improved from 35.78dB to 36.41 dB and 36.16dB for the 3×3 and 5×5 cases, respectively. For these two methods, the result with the second method is better than that with the first method. This is a topic that is still under investigation.

5. CONCLUSION

From the simulations, two things can be derived. The first is the effect of the spectrum. The case with long spectrum is that the result with ideal spectrum is better than that with estimated spectrum. But, more important thing is that the processing length is of consequence. The case with one point is better than that with the long spectrum. These are the two major factors that are investigated in this paper about Wiener filter. In all the cases, we do find out that adaptive Wiener filtering technique can effectively reduce the quantization error. This effect is more apparent for the first few subbands in subband image coder. There are still something that is to be investigated about the fact that this technique is not very effective in the higher band. For the higher band, since the coefficient is often quantized to zero, the varriance of the quantization error is equal to that of the coefficient, which is usually low compared to the lower band. Therefore, for a DCT image coder adopting uniform scalar quantizers, the use of adaptive Wiener filter in the quantized subbands can effectivelly reduce the quantization noise and increase the overall reconstruction performance.

6. REFERENCES

[1] J. S. Lim, *Two-Dimensional Signal and Image Processing.* Prentice Hall, 1990.

[2] Jelena Kovacevic, "Subband Coding Systems Incorporating Quantizer Models," *IEEE Trans. Image Processing*, vol. 4, no. 5, pp. 543--553, May 1995.

[3] Michael G. Strintzis and Dimitrios Tzovaras, "Optimal Construction of Subband Coders Using Lloyd-Max Quantizers," *IEEE Trans. Image Processing*, vol. 7, no. 5, pp. 649--667, May 1998.

[4] Wei Li, Olivier Egger and Murat Kunt, "Efficient Quantization Noise Reduction Device for Subband Image Coding Schemes," in *Proc. ICASSP*, 1995, pp. 2209--2212

[5] L.G. Roberts, "Picture Coding Using Pseudo-random Noise," *IRE Trans. on Information Theory*, Vol. IT--8, pp. 145--154, Feb. 1962.

[6] Karine Gosse and Pierre Duhamel, "Perfect Reconstruction versus MMSE Filter Banks in Source Coding," *IEEE Trans. Signal Processing*, vol. 45, no. 9, pp. 2188--2202, Sep. 1997.

[7] Hyun Wook Park and Yung Lyul Lee, "A postprocessing Method for Reducing Quantization Effects in Low Bit-Rate Moving Picture Coding," *IEEE Trans. Circ. Syst. Video Technol.*, vol. 9, no. 1, pp. 161--171, Feb. 1999.

[8] S. Minami and A. Zakhor, "An optimization Approach for Removing Blocking Effects in Transform Coding," *IEEE Trans. Circ. Syst. Video Technol.*, vol.5 no.2, pp. 74--82, Apr. 1995.

[9] Thomas Sikora and Hui Li, "Optimal Block-Overlapping Synthesis Transforms for Coding Images and Video at Very Low Bitrates", *IEEE Trans. Circ. Syst. Video Technol.*, vol.6, no.2, pp.157--167, Apr.1996.

[10] J. S. Lee, "Digital image enhancement and noise filtering by use of local statistics," *IEEE Trans. Patt. Ana. Mach. Int.*, Vol. PAMI--2, Mar.1980, pp. 165--168.

[11] N.S. Jayant and P. Noll, *Digital Coding of Waveforms.* Englewood Cliff NJ, Prentice Hall, 1984.

Table 1: PSNR comparison for image "lenna"

Quant. Scale factor	Window Size	Without Processing	Estimated spectrum	Ideal signal spectrum
1	3*3	35.7846	36.0455	36.0939
	5*5		36.0614	36.2242
	7*7		36.0915	36.2804
2	3*3	33.6918	33.9445	33.9339
	5*5		33.9489	33.8268
	7*7		34.0262	33.8470
3	3*3	32.3162	32.5518	32.1950
	5*5		32.5883	32.0478
	7*7		32.5807	32.0850
4	3*3	31.2420	31.4670	30.6940
	5*5		31.5125	30.5492
	7*7		31.3105	30.6068

Table 2: PSNR comparison for image "baboon"

Quant. scale factor	Window Size	Without Processing	Estimated spectrum	Ideal signal spectrum
1	3*3	27.7757	28.0092	28.3970
	5*5		27.9617	28.4602
	7*7		27.8875	28.4102
2	3*3	25.7307	25.9200	26.1328
	5*5		25.9083	26.1796
	7*7		25.8800	26.1881
3	3*3	24.7483	24.9379	25.0621
	5*5		24.9233	25.0820
	7*7		24.9057	25.0828
4	3*3	24.0792	24.2600	24.2916
	5*5		24.2417	24.2908
	7*7		24.1907	24.2894

Table 3: PSNR comparison for image "pepper"

Quant. scale factor	Window Size	Without Processing	Estimated spectrum	Ideal signal spectrum
1	3*3	34.7710	34.9688	35.0843
	5*5		34.9486	35.0301
	7*7		34.9763	35.0754
2	3*3	33.0589	33.2363	33.1214
	5*5		33.2530	33.0730
	7*7		33.2870	33.0580
3	3*3	31.8785	32.0494	31.6776
	5*5		32.0866	31.5827
	7*7		32.0559	31.5666
4	3*3	30.9413	31.1117	30.4111
	5*5		31.1537	30.2913
	7*7		30.9469	30.2871

Table 4. Error variance changes for each subband after noise reduction for the case of uniform scalar quantizer.

coef.	3×3	5×5	Coef.	3×3	5×5
0	-6.9	-7.16	32	-19.58	-10.51
1	-8.47	-8.35	33	-22.22	-7.69
2	-14.58	-17.03	34	-9.30	0.30
3	-13.88	-13.44	35	-0.57	0.30
4	-14.65	-14.35	36	-2.07	1.13
5	-10.03	-8.55	37	-8.95	1.64
6	-22.54	-22.29	38	-10.96	0.18
7	-13.73	-13.27	39	-14.87	-6.18
8	-12.52	-11.97	40	-8.10	1.58
9	-18.55	-19.88	41	-8.88	0.54
10	-15.73	-17.61	42	-6.61	-0.95
11	-18.32	-18.66	43	-4.17	-9.01
12	-15.57	-14.58	44	-4.77	-0.14
13	-17.40	-17.50	45	-3.60	0.80
14	-19.82	-20.06	46	-4.97	-0.04
15	-23.86	-16.98	47	-5.55	0.41
16	-17.21	-16.27	48	-1.15	0.95
17	-16.61	-14.44	49	-2.22	0.26
18	-11.72	-10.94	50	-1.70	-0.10
19	-18.21	-18.12	51	-1.50	0.07
20	-18.03	-16.09	52	-0.77	0.16
21	-10.53	-2.29	53	-0.49	0.35
22	-21.17	-12.65	54	-0.17	-0.15
23	-23.93	-17.40	55	-0.21	0.11
24	-18.65	-14.41	56	-0.51	-0.32
25	-20.29	-13.36	57	-0.78	-0.17
26	-21.83	-11.81	58	-0.29	-0.76
27	-19.78	-7.08	59	0.19	0.00
28	-8.11	1.01	60	-0.10	-0.12
29	-15.36	-3.21	61	-0.08	-0.04
30	-24.63	-14.32	62	-0.04	0.00
31	-20.17	-9.85	63	0.03	0.05

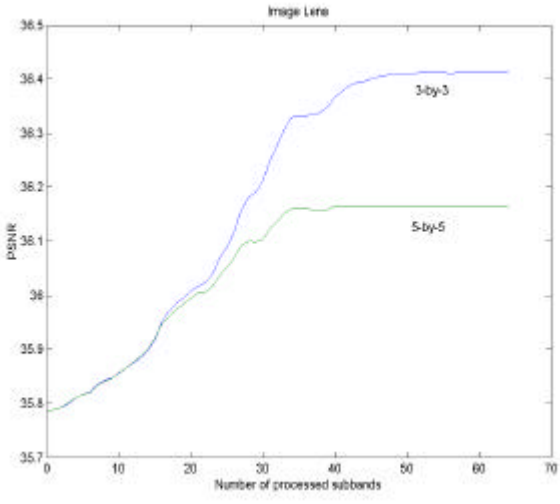

Figure 1. Reconstructed PSNR versus the number of processed subbands for image Lenna**.**